Temperature and Wavelength tuning of 2nd, 3rd and 4th harmonic generation in a two dimensional hexagonally poled nonlinear crystal

N. G. R. Broderick,* R. T. Bratfalean†, T. M. Monro, and D. J. Richardson

Optoelectronics Research Centre, University of Southampton, Southampton, SO17 1BJ, UK.

Phone: +44 (0)2380 593144, Fax: +44 (0)2380 593142

C. Martijn de Sterke

School of Physics, University of Sydney, Sydney, NSW, Australia

Using high power nanosecond pulses we measured the 2nd harmonic conversion efficiency of 2D hexagonally poled lithium niobate (HeXLN) as a function of temperature and wavelength. These results are compared with theoretical estimates and with measurements in 1D periodically poled lithium niobate. We find that for a substantial range of parameters a 2D non-collinear interaction has a broader tuning response than a 1D collinear interaction. We also observed and characterised third and fourth harmonic generation processes in the same crystal.

OCIS codes: 190.2620,190.4400,190.4160

1 Introduction

The idea of quasi-phase matching (QPM) a nonlinear process by periodically inverting the nonlinearity has a long and venerable history since it was first suggested by Armstrong *et al.*[1]. QPM allows highly dispersive materials which also have a high nonlinearity to be used in nonlinear experiments since the period of the nonlinear grating can be tailored to phase-match the desired nonlinear interaction. In addition QPM, as opposed to birefringent phase matching, allows the largest nonlinear coefficients of a material to be used, which are usually the coefficients for co-polarised interactions. Originally the concept of QPM was restricted to one-dimensional geometries such as periodically poled

†On leave from Babes-Bolyai University, Cluj-Napoca, Romania
*Electronic address: ngb@orc.soton.ac.uk

lithium niobate (PPLN) but lately a number of researchers have looked at varying the nonlinearity in the transverse dimensions both aperiodically[2] and periodically[3]. Berger examined theoretically nonlinear photonic crystals (NPCs) in which the nonlinearity varied periodically in two or three dimensions. In a NPC quasi-phase matching may be obtained in any direction where there is a suitable reciprocal lattice vector[3]. Recently we observed non-collinear 2nd harmonic generation in two dimensional hexagonally poled lithium niobate (HeXLN)[4] and observed efficiencies as high as 80%. In addition we examined the angular tuning of the HeXLN crystal and found it agreed well with theory. Since then researchers have looked at simultaneous wavelength conversion in a 2D NPC both theoretically[5] and experimentally[6] while others have looked theoretically at simultaneous multiple order harmonic generation in such crystals[7,8].

Our original experiments were performed using a high power picosecond fibre laser at 1531nm[9] as the fundamental to pump the crystal. Due to the nature of the source we were unable to vary its wavelength and so only the temperature and angle tuning of the SHG were measured. We observed a large temperature tuning bandwidth of $\sim 25°C$ for 2nd harmonic generation whereas in comparision a perfect PPLN crystal with the same length and period would have a bandwidth of $\sim 3°C$. The precise reason for this increased bandwidth is not known and analysis of these experimental results is complicated by the bandwidth of the source, the large peak conversion efficiency and the walk-off between the pump and the 2nd harmonic. In order to obtain a better understanding of the mechanisms involved we have now performed similar measurements in the weak conversion regime using a low power, nanosecond wavelength tunable source on a HeXLN crystal. These results are compared with the results of a direct numerical simulation and with a collinear interaction in PPLN performed using the same setup. In addition while performing these measurements we noted the generation of multiple green (3rd harmonic) and blue (4th harmonic) beams. We characterise these beams and show that they are due to two step processes phased matched by two different reciprocial lattice vectors (RLVs) in the crystal. The observation of multiple harmonics in HeXLN, demonstrates the enhanced opportunities for simultaneous phase matching of multiple nonlinear interactions in a NPC as compared to a 1D crystal.

2 Theoretical description of second harmonic generation in periodic materials

The term nonlinear photonic crystal was introduced by Berger[3] to describe a crystal in which the linear refractive index is constant but whose 2nd order nonlinear susceptibility varies periodically. One such crystal is HeXLN as shown in Fig. 1 in which the light regions have a positive nonlinearity while the dark regions have a negative nonlinearity. As can be seen the poled hexagons are distributed periodically across the plane. The purpose of such a periodicity is to quasi-phase match (QPM) a nonlinear interaction by adding additional crystal momentum to the phase matching condition.

Although in this paper we will concentrate on sum frequency generation (including 2nd harmonic generation) but of course QPM can be used for any 2nd order nonlinear interaction such as optical parametric generation. To see how the phase-matching condition arises it is simplest to start with the Helmoltz equation for the slowly varying envelope of a plane wave at the second harmonic frequency 2ω : by the Helmholtz equation[3]

$$\mathbf{k}^{2\omega} \cdot \nabla E^{2\omega}(\mathbf{r}) = -2i\frac{\omega^2}{c^2}\chi^{(2)}(\mathbf{r})(E^{\omega})^2 e^{\left(i(\mathbf{k}^{2\omega}-2\mathbf{k}^{\omega})\cdot\mathbf{r}\right)} \tag{1}$$

where $E^{2\omega}$ is the slowly varying envelope of a plane wave at the second harmonic frequency 2ω with a wavevector $\mathbf{k}^{2\omega}$ and similarly for the fundamental wave at a frequency of ω with amplitude E^{ω} and wavevector $\mathbf{k}^{\omega}$. In Eq. (1) the nonlinearity is represented by $\chi^{(2)}(\mathbf{r})$ which is here assumed periodic. To obtain this result we used the undepleted pump approximation[10], according to which the field at the fundamental frequency depends only on the linear properties of the structure and is unaffected by the nonlinearity. This is justified when the conversion efficiency to the second harmonic is small. In this approximation, the fundamental field simply acts as a known source for the field at the second harmonic, as in Eq. (1).

From Eq. (1) it can be seen that the intensity of the second harmonic is likely to remain small unless the exponent $(\mathbf{k}^{2\omega} - 2\mathbf{k}^{\omega}) \cdot \mathbf{r} \approx 0$. In general, due to dispersion, this is not the case and hence we must add an additional term to the exponent in order to assure that it is identically zero. Since the nonlinear susceptibility tensor $\chi^{(2)}$ is periodic we can write it as a Fourier series:

$$\chi^{(2)}(\mathbf{r}) = \sum_{n,m} \kappa_{n,m} e^{i\mathbf{G}_{n,m}\cdot\mathbf{r}}, \quad n, m \in \mathbb{Z}, \tag{2}$$

where $\mathbf{G}(n,m) = \mathbf{G}_{n,m}$ are the reciprocal lattice vectors of the structure and $\kappa_{n,m}$ are the corresponding Fourier coefficients[11]. Substituting Eq. (2) into Eq. (1) we now find a new phase matching condition,

$$\mathbf{k}^{2\omega} - 2\mathbf{k}^{\omega} - \mathbf{G}_{n,m} = 0, \tag{3}$$

must be satisfied for the interaction to proceed. Note that Eq. (3) also determines the angle (or angles) at which the 2nd harmonic is emitted from the crystal. The Fourier coefficient $\kappa_{n,m}$ then determines the strength of an interaction phase matched by $\mathbf{G}_{n,m}$ and if $\kappa_{n,m} = 0$ then the interaction will not occur. The attraction of using NPC's comes from the fact that Eq. (3) can be used as the defining condition for $\mathbf{G}_{n,m}$ and thus we can design our lattice to phase match the desired nonlinear interaction or nonlinear interactions. Similarly by altering the shape of the poled region within the unit cell we can adjust the relative ratios of the Fourier coefficients so that some nonlinear interactions are stronger than others. This ability to tailor the size of the Fourier coefficients becomes increasingly important

when using higher order RLVs as in general their associated Fourier coefficients are smaller than lower order RLVs. It should be pointed out that within a 2D geometry there is a much greater fabrication freedom than in 1D for changing the relative sizes of the Fourier coefficients by changing either the lattice or the shape of the poled region. This could allow simultaneous nonlinear interactions such as cascaded high harmonic generation to have a greater efficiency in 2D than 1D. We will return to this point in the final section of the paper.

All of the results presented in this paper were done using the NPC shown in Fig. 1 and so it behooves us to discuss here the properties of a hexagonal lattice. A hexagonal lattice with period a has basis vectors $\mathbf{b}_1 = a(1,0)$ and $\mathbf{b}_2 = a(1/2, \sqrt{3}/2)$ and the corresponding reciprocal lattice vectors (RLVs) are $\mathbf{G}_{n,m} = n\mathbf{e}_1 + m\mathbf{e}_2$ where $\mathbf{e}_{1,2}$ are the basis vectors for the reciprocal lattice, which is a hexagonal lattice with a period of $4\pi/(\sqrt{3}a)$ rotated by $\pi/2$ compared to the real space lattice as shown in Fig. 1. Note that the RLVs are longer by a factor of $2/\sqrt{3}$ compared to the RLVs for a 1D pattern with the same period. In the subsequent experiments we measured the 2nd harmonic conversion efficiency for a QPM process involving the RLV $G_{0,1}$. The associated Fourier coefficient $\kappa_{0,1}$ for this RLV is $3/\pi^2 = 0.30$. By comparison the Fourier coefficient for a 1D PPLN crystal with a mark to space ratio of 1:1 is $2/\pi = 0.64$. Thus under similar experimental conditions a 1D PPLN crystal will have a greater peak 2nd harmonic conversion efficiency than a 2D HeXLN crystal by a factor given by the ratio of the associated Fourier coefficients squared, which is ~ 4. Lastly we note that for our designed lattice with a hexagonally shaped poled region comprising 25% of the unit cell all even order Fourier coefficients should be identically zero and hence we would not expect to observe any interactions phase matched with even order RLVs.

3 Experimental Results

The hexagonal structure of our 2D NPC is shown in Fig. 1. This structure was revealed by lightly etching the sample in acid. Each hexagon is a region of domain inverted material - the total inverted area comprises 25% of the overall sample area. The fabrication procedure for this crystal is identical to that for PPLN except that a 2D patterned mask is used rather than a standard 1D mask. The crystal was 0.3mm thick and the hexagonal pattern was found to be uniform across the sample dimensions of 10 × 7mm (x-y) and was faithfully reproduced on the +z face. Lastly we polished the $\pm x$ -faces of the HeXLN crystal allowing a propagation length of 10mm through the crystal in the ΓM direction (see Fig. 1). Our HeXLN crystal has a period of 18.05 μm: suitable for non-collinear frequency doubling of 1536nm in the ΓM direction at 120°C using the RLV lattice vector $G_{0,1}$ (an elevated temperature was chosen to eliminate any potential photorefractive effects). As no additional fabrication steps are required to pole a 2D pattern as compared to a 1D pattern it should be straightforward to pole more complicated 2D patterns in lithium niobate

provided that the domain boundaries line up with the crystal axes. In addition we have found experimentally that finer periods can be achieved by poling hexagons than by poling long lines such as you need for PPLN Hence HeXLN like structures could be used for frequency doubling applications in the visible.

To investigate the properties of the HeXLN crystal we proceeded as follows. The HeXLN crystal was placed in an oven and mounted on a rotation stage which could be rotated by $\pm 15°$ around the z-axis while still allowing light to enter through the $+x$ face of the crystal. The fundamental pump beam consisted of 5ns transform limited square pulses obtained from a high power all-fibre cascaded amplification system[12] operating at a pulse repetition rate of between 50kHz and 2kHz. The wavelength of the source could be varied continuously in the range 1520nm-1560nm and had a measured bandwidth of < 3GHz which was sufficient to resolve the spectral features of the crystal's response. At the lowest repetition rate the peak pulse power was $\sim$ 20kW and this decreased as the repetition rate increased. The output from the amplifier was weakly focused into the HeXLN crystal using a 17cm focal length lens giving a focal spot diameter of 150μm (corresponding to a depth of focus of $\sim$9mm) and a corresponding peak intensity of $> 5\text{MW/cm}^2$. Note that in our experimental configuration a zero angle of incidence corresponds to propagation along the ΓM direction in the Brillouin zone while the nearest RLVs are in the ΓK directions. For our crystal the response should be symmetrical under rotation about the ΓM axis and indeed we observed that this was the case. By measuring the angle that the crystal had to be rotated to obtain two symmetrical outputs the location of the ΓM axis could be determined and all of the angles reported here refer to deviations from the ΓM axis. For these experiments the input angle was $\sim 2°$ which was optimised for maximum 2nd harmonic generation using $G_{0,1}$[4]. The output in these experiments consisted of a 2nd harmonic spot propagating at an angle of $\sim 0.5°$ relative to the remaining fundamental. In addition multiple green spots corresponding to sum frequency generation between the fundamental and 2nd harmonic were observed and at the highest powers (lowest repetition rates) we observed the appearance of two blue spots generated via two cascaded second harmonic processes. We now discuss in detail the 2nd harmonic spot before describing the higher order harmonics.

3.1 *Second Harmonic Generation*

Fig. 2 shows the temperature response of the 2nd harmonic external conversion efficiency for our crystal (solid line) for an input wavelength of 1536nm. In addition the short dashed line shows the theoretical prediction for the line shape of the crystal while the long dashed line shows the measured response for a PPLN crystal (which is described below). In order to facilitate a comparison between the responses all curves have been normalised to have unit efficiency while the x-axis records the temperature difference from ideal phase matching. Note that the theoretical and experimental

results agree remarkably well: the FWHM of the experimental curve is 8.5°C while the theoretical curve has a width of 9.0°C. Both experimental and theoretical curves are also distinctly not sinc-shaped which is the expected shape for a collinear interaction in PPLN. In order to determine whether or not this large width of the response was due to experimental conditions or intrinsic to the non-collinear nature of the interaction we repeated the experiment with a 12mm length of PPLN with the same period and with the same experimental conditions. For the PPLN crystal we observed a sinc shaped response as expected and with a FWHM of 3.5°C which agrees well with the theoretical value of 3°C and this is shown by the long dashed line in Fig. 2.

In Fig. 2 we have normalised the efficiency for both the HeXLN and PPLN curves whereas as mentioned earlier the ratio of the peak efficiencies for both curves should be ≈ 4 for low pump powers and we measured a ratio of 3.7 which is again in good agreement with the simple theory. Note that the actual efficiency in HeXLN is reduced slightly by the fact that the fundamental and SH are not copropagating and at the moment we are not able to estimate this effect analytically.

The theoretical curve in Fig. 2 was obtained by numerically solving the Helmholtz equation

$$\nabla^2 \mathcal{E}^{2\omega} + \frac{n_2^2(2\omega)^2}{c^2}\mathcal{E}^{2\omega} = \frac{(2\omega)^2}{c^2}\chi^{(2)}(\mathbf{r})\,(\mathcal{E}^{\omega})^2, \tag{4}$$

where $\mathcal{E}(\mathbf{r})$ has the full position dependence, using a Green function approach. Note that Eq. (1) is derived from Eq. (4) after make the usual paraxial approximation,[10] and was used in Section II as it highlights the importance of phase matching. However in our theoretical analysis we have chosen to use Eq. (4) since it is tractable to a Green function approach which brings some benefits as discussed below. For the two-dimensional Helmholtz equation (4) the Green function is

$$G(\mathbf{r};\mathbf{r}') = -\frac{i}{4}H_0^{(1)}(k^{2\omega}|\mathbf{r}-\mathbf{r}'|), \tag{5}$$

where $H_0^{(1)}$ is the zeroth order Hankel function of the first kind. This Green function needs to be convolved with the source distribution on the right-hand side of Eq. (4), which, as discussed, in the low-conversion limit, can be found from the linear properties of the medium.

Now apart from the refractive index jump at the sample edges, the linear properties of the structure are uniform. In addition, for the experiments described here, beam diffraction is almost negligible, and the fundamental beam inside the structure can to a good approximation be described by a plane wave. Nonetheless, the theoretical results do include the full effects of diffraction.

In the far field, the Green function Eq. (5) can be approximated by its asymptotic expansion, the relevant position

dependence of which is $\exp(ik^{2\omega}|\mathbf{r}-\mathbf{r}'|)$. The final approximation that can be made is to use the Fraunhofer approximation in evaluating the factor $|\mathbf{r}-\mathbf{r}'|$, which is justified by the observation that the width of the beam is much smaller than the distance between the HeXLN crystal and the observation point. The eventual calculation is thus straightforward and comes down to adding the contributions of multiple point sources, each of which is proportional to the sign of the local nonlinearity and the square of the local electric field strength. This Green function approach has the attraction that no apriori assumptions about the direction of the second-harmonic beam need to be made, as all possible propagation directions are included in the calculation.

If one knows that only a single Fourier component is involved in the generation process then a variation on the procedure described above which includes only a single Fourier component in the distribution of the quadratic nonlinearity [Eq. (2)] can be used. This has the attraction that for a wide range of pump profiles the calculation can be done analytically.

The complete output of the theoretical calculations is shown in Fig. 3 which shows a contour plot of the 2nd harmonic conversion efficiency versus temperature and output angle. To obtain the curve in Fig. 2 we integrated over the output angle as this is what is done experimentally. Note from Fig. 3 that the effect of the noncollinear interaction is to tilt the usual sinc^2 response in the $T-\theta$ plane. In fact, it can be shown that

$$\frac{d\vartheta_o}{dT} = \frac{k_f' - (k_s'/2)\cos(\vartheta_i)}{k_s \sin(\vartheta_i)}, \tag{6}$$

where $k_{f,s}' = dk_{f,s}/dT$, ϑ_i is the incident angle of the fundamental beam with respect to the ΓM direction, and ϑ_o is the output angle of the second harmonic. Because of the tilt, after integrating over output angle, the sidelobes are smoothed out as in Fig. 2. The existence of the tilted sidelobes was confirmed directly by placing a CCD camera in the output beam and looking at the position of maximum 2nd harmonic generation as a function of the temperature. As expected from Fig. 3 as the temperature varied so did the position of the 2nd harmonic spot. For some temperatures, however, maximum 2nd harmonic intensity occurred in two closely spaced positions, which can be understood from Fig. 3. From this figure it can be seen that for a range of temperatures around 130°C, for example, the output is peaked at two distinct angles of around 1.9° and 2.1°, leading to the observation of two distinct spots.

It is well known that the wavelength response of a PPLN crystal has the same shape as the temperature response as in both cases the important parameter is the phase mismatch defined by the left hand side of Eq. (3) which is zero only for perfect phase matching. We measured the wavelength response of both the PPLN crystal and the HeXLN crystal and found them to be identical in shape to their respective temperature responses (after a suitable rescaling). As expected the wavelength response of the HeXLN crystal was again broader than that of the PPLN crystal by

about a factor of two. Similarly we have simulated the response of the crystal to different wavelengths and the shape of the response is the same as that shown in Fig. 3.

3.2 *Higher Order Harmonic Generation*

Two-dimensional periodically poled crystals, as opposed to one-dimensional ones, have RLVs along a variety of specific directions. This allows the simultaneous quasi-phase-matching of multiple nonlinear processes such as cascaded higher order harmonic generation. Apart from the 2nd harmonic of the 1536nm radiation we were also able to observe distinct green and blue beams emerging from our HeXLN crystal, which were cascaded 3rd and 4th harmonics, respectively. When measuring the temperature tuning bandwidth for the 2nd harmonic we used a relatively low input power to minimise the power in the higher order harmonics. However in this section we increased the input power by reducing the repetition rate of the source so as to increase the power in the higher order harmonics. We found that the conversion efficiency from the fundamental to the 2nd harmonic was typically above 20% and thus the undepleted pump assumption used in the earlier section cannot be used here. This can be seen in the broader bandwidths for the 2nd harmonic presented below. The 3rd harmonic is the sum frequency between the fundamental and the 2nd harmonic. The 4th harmonic is the result of two 2nd harmonic steps. The wavevectors involved in these processes are shown schematically in Fig. 4. By measuring the incidence angle of the infrared beam we were able to determine its propagation direction in the crystal and to identify the quasi-phase-matching RLVs involved in all the steps of the cascaded process. In their turn the RLVs were used to determine the propagation direction of the harmonics inside the crystal and their emerging directions. The results of our ray tracing simulation are in excellent agreement with the experimental observations and details of this analysis are presented in later sections.

In order to determine the RLVs involved in the generation of the higher order harmonics we used the modified Ewald construction as described by Berger[3]. In order to do this we needed to know accurately the angle between the ΓM axis of the crystal and the incoming fundamental. As discussed earlier this was detrmined due to the symmetry of the crystal about the ΓM axis. Hence we rotated the crystal and observed the angles for which symmetrical patterns appeared. In addition by looking at the back reflection of the fundamental from the front face of the crystal we found that the crystal ends faces were not exactly at 90^o degrees to the ΓM axis but instead at an angle of 89.5^o. Once the input angle of the fundamental was known then the output angles for a given nonlinear process could be calculated theoretically for the processes shown in Fig. 4 using the modified Ewald construction.

There were two types of cascaded 3rd harmonics, which we observed and measured. In the first case, which is the more usual one in lithium niobate, both steps of the process, the 2nd harmonic and the sum frequency mixing, are

mediated by the d_{33} coefficient of lithium niobate and such an interaction is refereed to as type I phase matching. In the second case we observed a type II nonlinear interaction in which the 2nd and 3rd harmonics are orthogonally polarised. Such a process is mediated by the d_{15} coefficient of lithium niobate[10] and can only be excited if the incident fundamental field has both horizontal and vertical components. We also observed that for the type II interaction the 3rd harmonic emerged with a horizontal polarisation whereas for the type I process the 3rd harmonic, was vertical polarised along with the fundamental and 2nd harmonic.

As far as the cascaded 4th harmonic is concerned both steps of the process were mediated by the d_{33} coefficient of lithium niobate and the beam emerges with a vertical polarisation. We will now discuss the different harmonic processes separately beginning with the third harmonic generation and ending with the 4th harmonic generation.

3.3 *Type I Third Harmonic Generation*

As described above when the crystal was illuminated with high power nanosecond pulses we observed the generation of multiple green beams (the 3rd harmonic of the fundamental). These beams were all emitted at different angles and the appearance of these beams depended on the input angle of the fundamental and the temperature and thus we believed that they were created by a cascaded process as shown in Fig. 4(a). The possibility that the beams were created via a single step process involving $\chi^{(3)}$ was discounted as the poling does not invert $\chi^{(3)}$ and hence it would not be quasi-phase-matched. In order to understand the process we decided to concentrate on a single green spot which was well isolated from the other green spots and measure both its temperature tuning as well as the angle that it was emitted at. The simultaneous temperature-tuning curves of the 2nd and 3rd harmonic in the 105°C to 180°C temperature range are shown in Fig. 5. The incidence angle of the fundamental beam was adjusted to make the 2nd harmonic intensity peak at around 126°C. The peak power of the input pulses was 2.8kW, providing a power density of approximately 16 MW/cm^2 and for this experiment we had a peak internal conversion efficiency of $> 40\%$. From the graph it can be seen that the peaks of the 2nd and 3rd harmonics occur at different temperatures. This indicates that the two processes are phase-matched at slightly different temperatures and this is one reason why the tuning curve for the 3rd harmonic has a greater width than the 2nd harmonic curve 26.1°C for the 3rd harmonic as compared to 14.9°C for the 2nd harmonic.

For the process depicted in Fig. 5 the fundamental wave propagated at an angle of 1.47^o degrees to the ΓM axis while the 2nd and 3rd harmonics propagated at angles of 0.80^o and -8.21^o respectively at a temperature of 126.26°C (the angles for the symmetrical spots were also measured but are not given here). From the measurement of the fundamental's angle of propagation we were able to determine that the RLVs involved were $G(0,1)$ for the first step

and $G(-10,12)$ for the 2nd step. Note that from the measured angles high order RLVs are predicted to be involved and importantly the Fourier coefficients for such RLVs are identically zero for our crystal design with a poled fraction of 25%. The fact that we observed emission at these angles suggests that the crystal was overpoled and indeed inspecting the crystal under a microscope suggests that the area of the poled regions is $\sim 3\%$ greater than expected. This value agrees with an earlier estimate based upon the relative intensity of the different 2nd harmonic spots[4].

Lastly we note that although the green spots appeared quite bright to the eye in fact very little power was actually present in the green beams. The main reasons for the low conversion efficiency are, we believe, the extremely small Fourier coefficient for the RLV involved and the angle between the 2nd harmonic and the fundamental which limited the interaction region. In addition, the fact that the 2nd and 3rd harmonics were phase matched at different temperatures also results in a reduction of the peak efficiency. A "back of the envelope" calculation for the efficiency of the 3rd harmonic can be performed by assuming that the efficiency for the 3rd harmonic is proportional to the size of the appropriate Fourier coefficient ($\kappa_{10,-12}$) squared times the ratio of the 2nd harmonic power to the fundamental power[13]. Substituting in the appropriate numbers gives an expected peak 3rd harmonic power of $\sim$ 400nW which compares well with the measured peak power of $\sim$ 100nW with the difference being mostly due to uncertainties about the size of the Fourier coefficient [taken as $1/(10.12)$] for the purposes of this calculation. Such a calculation shows that when designing crystals for quasi-phase matching RLVs the geometry should be such that the size of the relevant Fourier coefficients are maximised. In final section of the paper we will discuss ways to improve the efficiency of such processes and instead now discuss the observation of a second type of green beam.

3.4 *Type II Third Harmonic Generation*

In the experimental setup we had inserted a half wave plate in front of the crystal in order to ensure that the fundamental beam was vertically polarised at the input to the crystal. This is as the poling process only inverts selected components of the 2nd order susceptibility tensor and thus the input light needs to be vertically polarised in order to observe 2nd harmonic generation. Interestingly while rotating the input plane of polarisation of the fundamental from vertical to horizontal we observed the appearance of an additional green beam. This was completely unexpected since if the green beam was being generated by a type I interaction then it would have a maximum efficiency when both the fundamental and 2nd harmonic beams were vertically polarised. We measured the polarisation of this additional green beam and found that it was orthogonally polarised to the 2nd harmonic and thus it was being created via a type II sum frequency interaction in which a horizontally polarised fundamental photon mixes with a vertically polarised 2nd harmonic photon to produce a horizontally polarised 3rd harmonic photon. This is we believe the first observation of

type II non-degenerate sum frequency generation in periodically poled lithium niobate and the fact that we managed to observe it dramatically illustrates the increased density of RLVs for a 2D crystal as compared to a 1D crystal. In addition the non-collinear nature of the process also meant that this green beam appeared in a previously dark region making it easy to spot.

Evidence for the type II nature of this green beam is shown in Fig. 6 which shows the measured 2nd and 3rd harmonic powers as the plane of polarisation of the fundamental is rotated from horizontal to vertical and back to horizontal. For these experiments the peak intensity of the fundamental was 12 MW/cm^2, while the incident angle was chosen so that the 2nd harmonic intensity peaked at 138°C In Fig. 6 the points represent the measured values while the lines represent the results from a simple 1-D model of the process. Note that for both the experimental points and the theoretical curve the third harmonic peaks at an incident angle of 37° from the vertical. As expected for a type I process involving the d_{33} tensor component the 2nd harmonic is a maximum when the fundamental is vertically polarised and the power in the 2nd harmonic beam depends strongly on the angle of the fundamental polarisation. The power in the green beam follows a very different trend to the 2nd harmonic being zero when the fundamental and 2nd harmonic are co-polarised and a maximum when the fundamental is polarised at an angle of 37° degrees from the vertical. Type II interactions find applications in process such as the production of entangled photons for quantum cryptography and in many cases increasing the efficiency of the process via QPM would be an advantage.

To obtain the solid curves in Fig. 6 we used a very simple 1-D model which assumed that all beams were propagating in the same direction and that the values of the nonlinearity for each interaction were identical. The results from this model were then scaled so that the peak height of the 2nd harmonic matched the experimental peak and the third harmonic was scaled by the same amount so that the ratio between the 2nd and 3rd harmonic power is the same in both experiment and theory. Given the simplistic nature of the model the level of agreement is quite surprising and importantly predicts the correct angular dependence for the 3rd harmonic. In the low conversion regime the angular dependence is expected to be a generic feature of type II processes and does not depend strongly on the relative sizes of the nonlinear coefficients. Using a more accurate two-dimensional model, along, with the correct sizes of the relative nonlinearity should give a better fit to these experimental results. We also measured simultaneously the temperature-tuning curves of the 2nd and 3rd harmonic and obtained a temperature tuning width of 9.06° for the 2nd harmonic and 4.31°C for the 3rd harmonic. By measuring the incident angle of the fundamental we were able to determine that the RLV involved in the type II process was either $G(2,3)$ or $G(3,2)$ depending on which side of the

ΓM axis the fundamental beam was located.

3.5 *Cascaded 4th harmonic process.*

The last process we characterised was the generation of blue light via a two step process as shown in Fig. 4b. Here two fundamental pump photons combine to produce a 2nd harmonic photon and then two 2nd harmonic photons combine to produce a single 4th harmonic photon. The temperature tuning curves for these processes are shown in Fig. 7. The peak power of the pulses was 2.4kW, providing a power density of approximately 14 MW/cm^2. We adjusted the incidence angle of the fundamental to maximise the 2nd harmonic signal around 158°C as it was found that this temperature gave the maximum conversion efficiency for the 4th harmonic. In contrast to the previous two cascaded processes, we were able to identify two distinct 4th harmonic beams for the same angle of incidence of the fundamental beam. The intensities of these two 4th harmonic beams were only slightly different but we measured the temperature-tuning curve only for the most intense one, which we consider to be the main. The widths of the temperature-tuning curves are 26.4°C for the 2nd harmonic and 13.0°C for the 4th harmonic. Note that the power of the blue spots is higher by about a factor of 8 relative to the type I third harmonic process. This allows us to be confident that the blue light is generated by a two step process and not a three step process involving the 3rd harmonic.

For these measurements the internal angle of the fundamental relative to the ΓM axis was 0.61^o while the 2nd harmonic propagated at an angle of -0.05^o. The two blue beams propagated at angles of -5.98^o and 5.89^o relative to the ΓM axis. Using the modified Ewald construction we initially obtained quite poor agreement between the measured and predicted angles for the 4th harmonic. A possible reason for this was an error in the predicted value of the refractive index at $384nm$ which gave the wrong size of the k-vector for the 4th harmonic. Altering the refractive index of the 4th harmonic in turns alters the length of the 4th harmonic k-vector. However due to the discrete positions of the RLVs the refractive index can only be altered in discrete steps while still maintaining the phase-matching condition. We found that the smallest possible increase was 0.18% which raised the refractive index at 384nm from 2.36516 to 2.36945. This increase allowed a different RLV was used in the Ewald construction giving a much better agreement between theoretical and experimental angles. The initial values of the refractive index were obtained from the Sellmeier equations for PPLN given by Jundt[14] and these values were obtained using results in the frequency range from 404nm-3000nm. Increasing the frequency increases the error in the Sellmeier equations since high frequencies are closer to the absorption edge of lithium niobate. Thus we believe that the most significant source of the error between the modelling and experiment was the refractive index. After making these changes the RLVs

involved were identified as $G(-6,14)$ and $G(14,-6)$.

4 Discussion and Conclusions

In the literature on periodically poled nonlinear materials an enduring theme has been looking at schemes for the generation of the third harmonic of a pump beam. Typically in PPLN this is done in two separate crystals, the first of which is designed to double the pump while the second crystal which has a different period is designed for sum frequency generation between the fundamental and the second harmonic. Such a scheme suffers from the disadvantage that it can only operate in one direction and secondly it is more difficult to align than a process involving only a single crystal. More recently some authors have suggested using a poled pattern based on the Fibonacci series to allow both processes to occur simultaneously in a single crystal[15,16]. Theoretically having both processes occurring simultaneously can be more efficient than when they occur separately however in the case of a Fibonacci lattice this increase in efficiency does not compensate for the reduction in size of the appropriate Fourier coefficients. Since Berger's original work describing NPCs a number of authors have pointed out that a NPC can be used to phase match two simultaneous nonlinear interactions[5,7,8]. Essentially one quasi-phase matchs the first interaction using one of the basis vectors for the reciprocal lattice and then the second interaction can be quasi-phase matched using the 2nd basis vector as it is assumed that these can be chosen independently.

The first experimental proof of the suitability of a NPC to phase match multiple interactions was performed earlier by Chowdhury *et al.*[6] who observed simultaneous optical wavelength conversion in a NPC, while we have presented here the first observations of simultaneous multiple harmonic generation in a NPC. Although none of these experimental results were not particularly efficient they do demonstrate the suitability of using NPCs for simultaneous phase-matching of multiple nonlinear interactions. In particular the fact that we were able to observe 3rd and 4th harmonic generation despite the fact that we had not designed the crystal with this in mind illustrates the potential that NPCs have in this area. In our experiments these higher order processes were phase matched by high order RLVs [$G(10,-12)$ and $G(6,14)$] and therefore the size of the the associated Fourier coefficients were quite small resulting in the low efficiencies measured. In this section we briefly discuss the problem of optimising the lattice structure for either third or 4th harmonic generation via cascaded processes.

The problem of third and fourth harmonic generation in nonlinear photonic crystals has been treated theoretically by a number of authors who have shown that in general an infinite number of possible lattices can be used. Thus the important question is which lattice gives the best efficiency and this is still we believe an open question. For a realistic geometry there are two important factors which limit the efficiency – the first is the angles between the

propagation directions of the various beams and the second is the size of the relevant Fourier coefficient. Clearly minimising the angles involved increases the effective interaction region and hence the overall efficiency. Thus ideally we would want all the processes to be collinear but this is not possible in PPLN and hence non-collinear geometries must be considered. Similarly increasing the relevant Fourier coefficients will increase the efficiency. For the simple structures which can be easily fabricated the Fourier coefficients decrease like $1/(n.m)$ and hence we would like to use the smallest possible RLVs to phase match the interactions[17]. However the fabrication process constrains the period of the crystals to be above $\sim 7\mu$m and so in realistic situations higher order RLVs must be used.

In order to improve the efficiency of the 3rd and 4th harmonic generation we have examined numerically a large number of possible lattices to determine which geometries would give the smallest angles and largest Fourier coefficients. Furthermore we have only consider lattices that we can actually fabricate in lithium niobate. By going to a lattice structure in which the size of the two lattice vectors are different we have found that it is possible to obtain simultaneous phase-matching of either 2nd and 3rd harmonic or 2nd and 4th harmonic using the reciprocal lattice vectors $G(1,0)$ for the 2nd harmonic and $G(0,3)$ for either the third or fourth harmonic. Furthermore for these lattices the angles between the various beams is less than 3^o ensuring a large interaction region. Repeating the back of the envelope calculation performed earlier suggests that for a hexagonally shaped poled region using $G(0,3)$ rather than $G(10,12)$ should increase the efficiency of the third harmonic generation process by a factor of almost 2000. This represents a significant increase and highlights the need for correctly designing the crystal. We are currently fabricating new masks based on these patterns and hope that in the near future we should be able to observe high efficiency third and 4th harmonic generation in 2D NPCs.

These results presented here show that two dimensional nonlinear crystals such as HeXLN are highly suited for the simultaneous phase-matching of multiple nonlinear interactions. In addition they compare favourablely with PPLN for second harmonic generation in terms of their bandwidth. This is due to both the non-collinear nature of the interactions which results in a broader bandwidth and the wealth of reciprocal lattice vectors present. This greater density of RLVs also lead to the observation of type II non-degenerate sum frequency generation and we believe that this is the first time that such a process has been observed in periodically poled lithium niobate.

Using a Green function approach we have modelled the second harmonic generation process in our crystal for the undepleted pump regime and found that it is in excellent agreement with the experimental results. Lastly we have investigated different designs for 2D nonlinear photonic crystals with an aim of finding crystals which should have high efficiencies for third and 4th harmonic generation.

References

[1] J. A. Armstrong and *et al.*, Phys. Rev. **127,** 1918 (1962).

[2] G. Imeshev, M. Proctor, and M. M. Fejer, "Lateral patterning of nonlinear frequency conversion with transversely varying quasi-phase-matching gratings," Opt. Lett. **23,** 673–675 (1998).

[3] V. Berger, "Nonlinear Photonic Crystals," Phys. Rev. Lett. **81,** 4136–4139 (1998).

[4] N. G. R. Broderick, H. L. Offerhaus, G. W. Ross, D. J. Richardson, and D. C. Hanna, "HeXLN: A 2-Dimensional nonlinear periodic crystal," Phys. Rev. Lett. **84,** 4345–4348 (2000).

[5] A. Chowdhury, S. C. Hagness, and L. McCaughan, "Simultaneous optical wavelength interchange with a two-dimensional second-order nonlinear photonic crystal," Opt. Lett. **25,** 832–834 (2000).

[6] A. Chowdhury, C. Staus, B. F. Boland, T. F. Kuech, and L. McCaughan, "Experimental demonstration of 1535-1555nm simultaneous optical wavelength interchange with a nonlinear photonic crystal," Opt. Lett. **26,** 1353–1355 (2001).

[7] C. M. de Sterke, S. M. Saltiel, and Y. S. Kivshar, "Efficient collinear fourth-harmonic generation by two-channel multistep cascading in a single two-dimensional nonlinear photonic crystal," Opt. Lett. **26,** 539–541 (2001).

[8] S. M. Saltiel and Y. S. Kivshar, "Phase matching in nonlinear $\chi^{(2)}$ photonic crystals," Opt. Lett. **25,** 1204–1206 (2000).

[9] N. G. R. Broderick, D. J. Richardson, D. Taverner, and M. Ibsen, "High power chirped pulse all-fibre amplification system based on large mode area fibre components," Opt. Lett **24,** 566–568 (1999).

[10] R. W. Boyd, *Nonlinear Optics* (Academic, San Diego, 1992).

[11] C. Kittel, *Introduction to Solid State Physics*, 3rd ed. (John Wiley and Sons, New York, 1953).

[12] D. Taverner, D. J. Richardson, L. Dong, J. E. Caplen, K. Williams, and R. V. Penty, "158 μJ pulses from a single transverse mode, large mode-area EDFA," Opt. Lett. **22,** 378–380 (1997).

[13] Such a calculation should not be taken too seriously but it does give a very rough order of magnitude calculation for the efficiencies.

[14] D. H. Jundt, "Temperature-dependent Sellmeier equation for the index of refraction, ne, in congruent lithium niobate," Opt. Lett. **22,** 1553–1555 (1997).

[15] S. ning Zhu, Y. yuan Zhu, Y. qiang Qin, H. feng Weng, C. zhen Ge, and N. ben Ming, "Experimental Realization of Second Harmonic Generation in a Fibonacci Optical Superlattice of $LiTaO_3$," Phys. Rev. Lett. **78,** 2752–2755 (1997).

[16] C. Zhang, H. Wei, Y.-Y. Zhu, H.-T. Wang, S.-N. Zhu, and N.-B. Ming, "Third-harmonic generation in a general two-component quasi-periodic optical superlattice," Opt. Lett. **26,** 899–901 (2001).

[17] One can of course design crystals in which any desired Fourier coefficients are maximised however such crystals are likely to contain fine features which are not easily fabricated. Our decision to look only at low order Fourier components is based on the fact that the resulting patterns are easily fabricated.

Figures

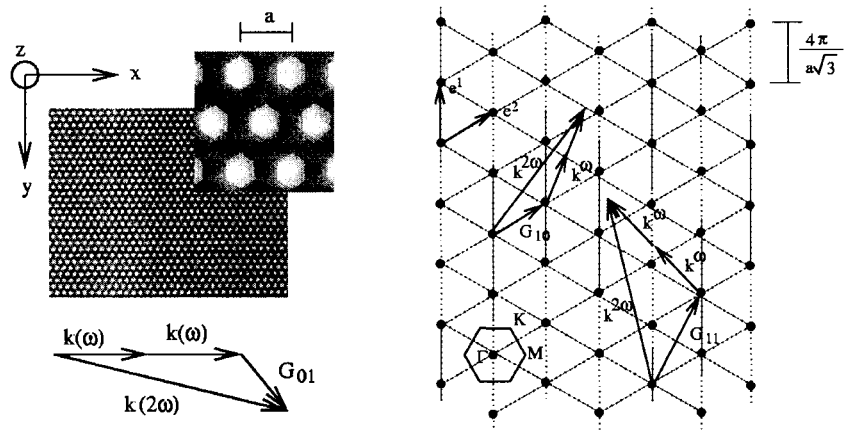

FIG. 1: (a) Picture of the HeXLN crystal and wave vectors involved in the SHG process. The period a of the crystal is 18.05μm is as shown in the picture and is uniform over the whole sample. In our experiments propagation was in the $+x$ direction. Fig. b shows the reciprocal lattice for our crystal along with possible examples of SHG using different RLVs. Note that propagation in the ΓM direction corresponds to propagation in the $+x$ direction.

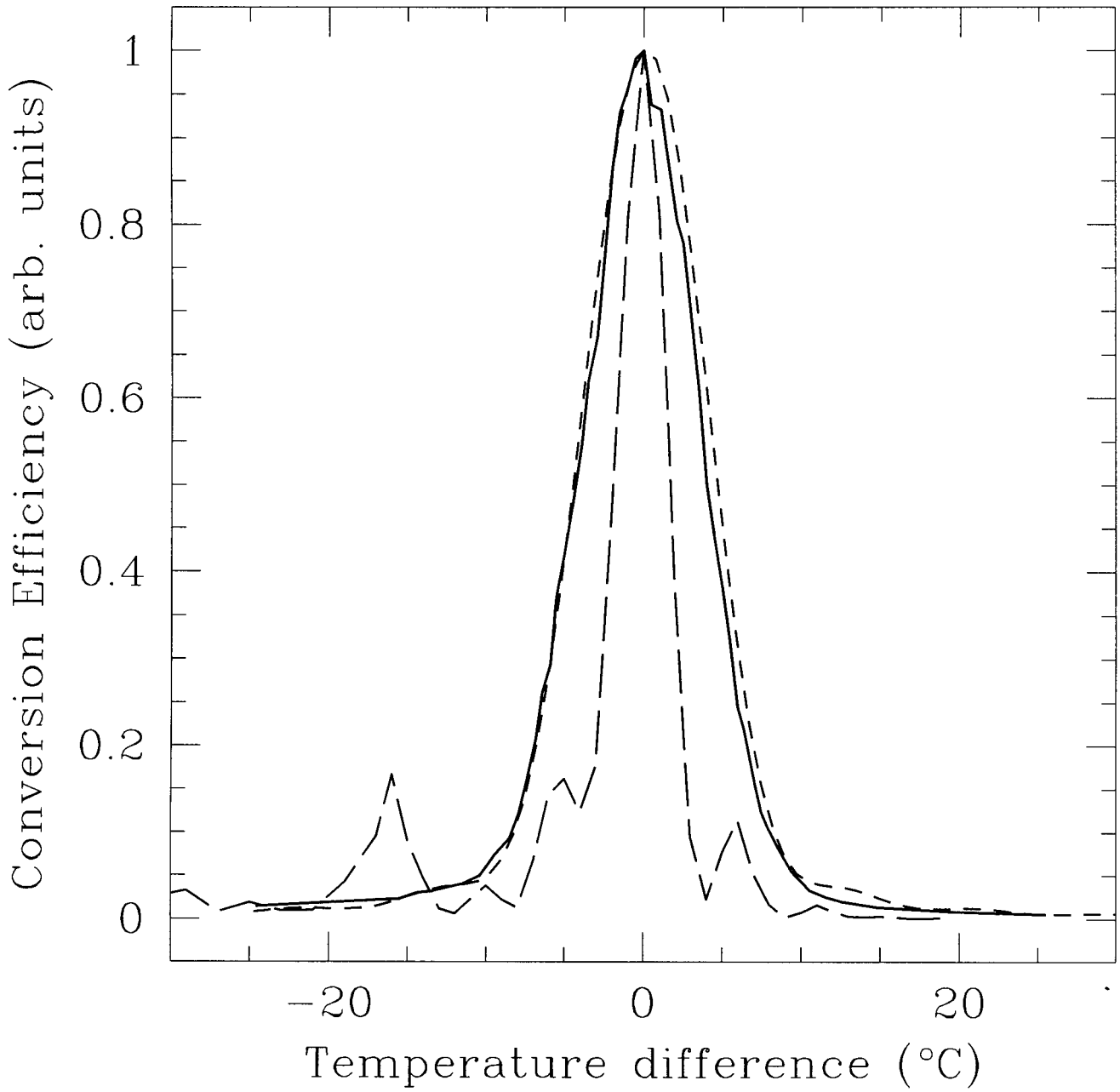

FIG. 2: The temperature dependence of the NPCs are shown above. The solid line is the measured efficiency curve for the HeXLN crystal, the long dashed line is the measured PPLN response and the short dashed line is the theoretical efficiency for HeXLN.

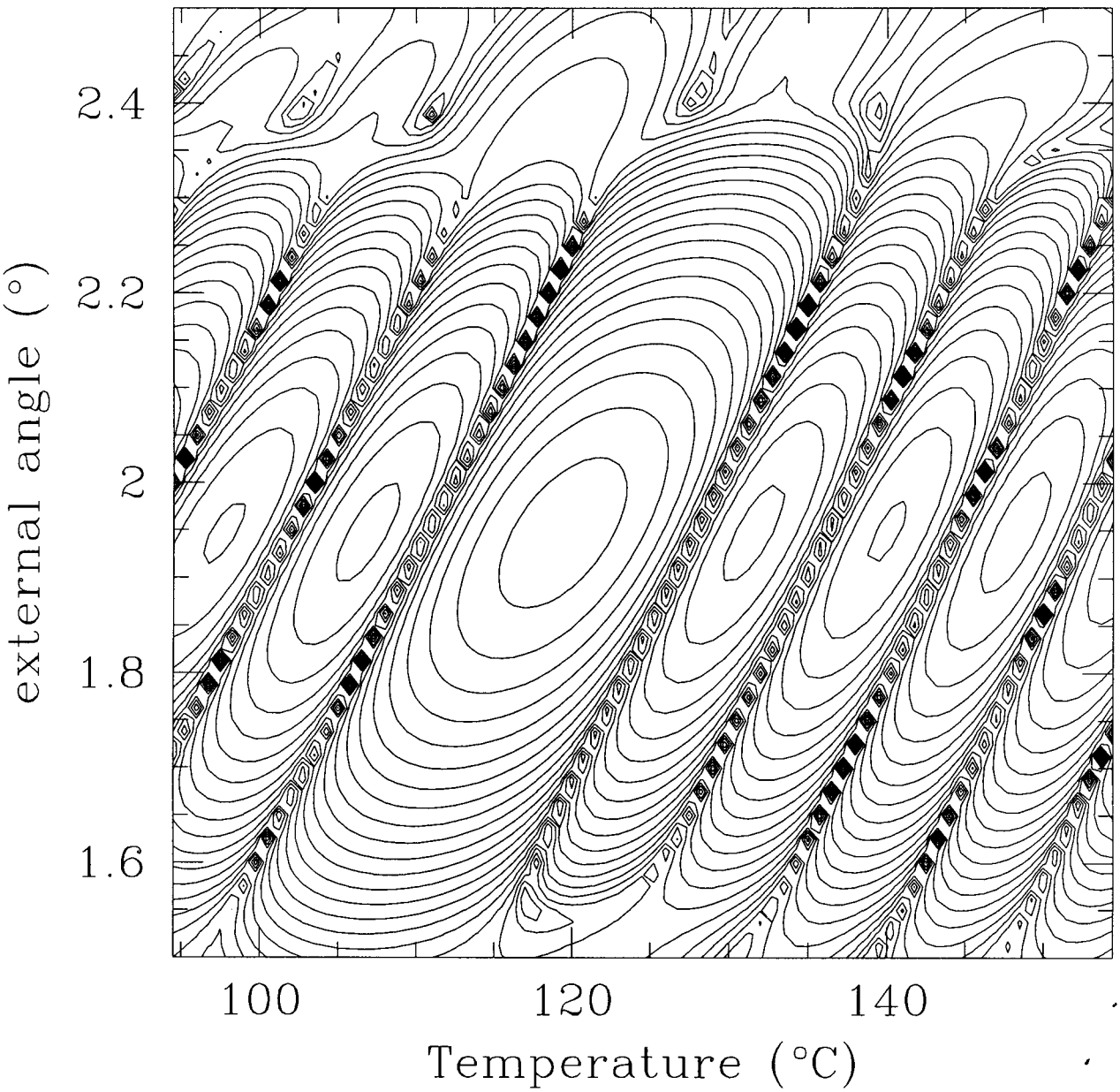

FIG. 3: Contour plot of the 2nd harmonic conversion efficiency against temperature and output angle.

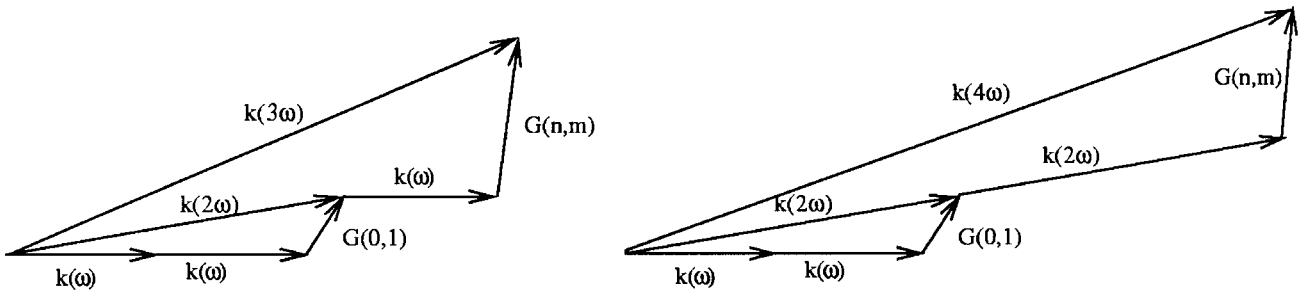

FIG. 4: Quasi-Phase matching diagrams for the cascaded generation of 3rd and 4th harmonics.

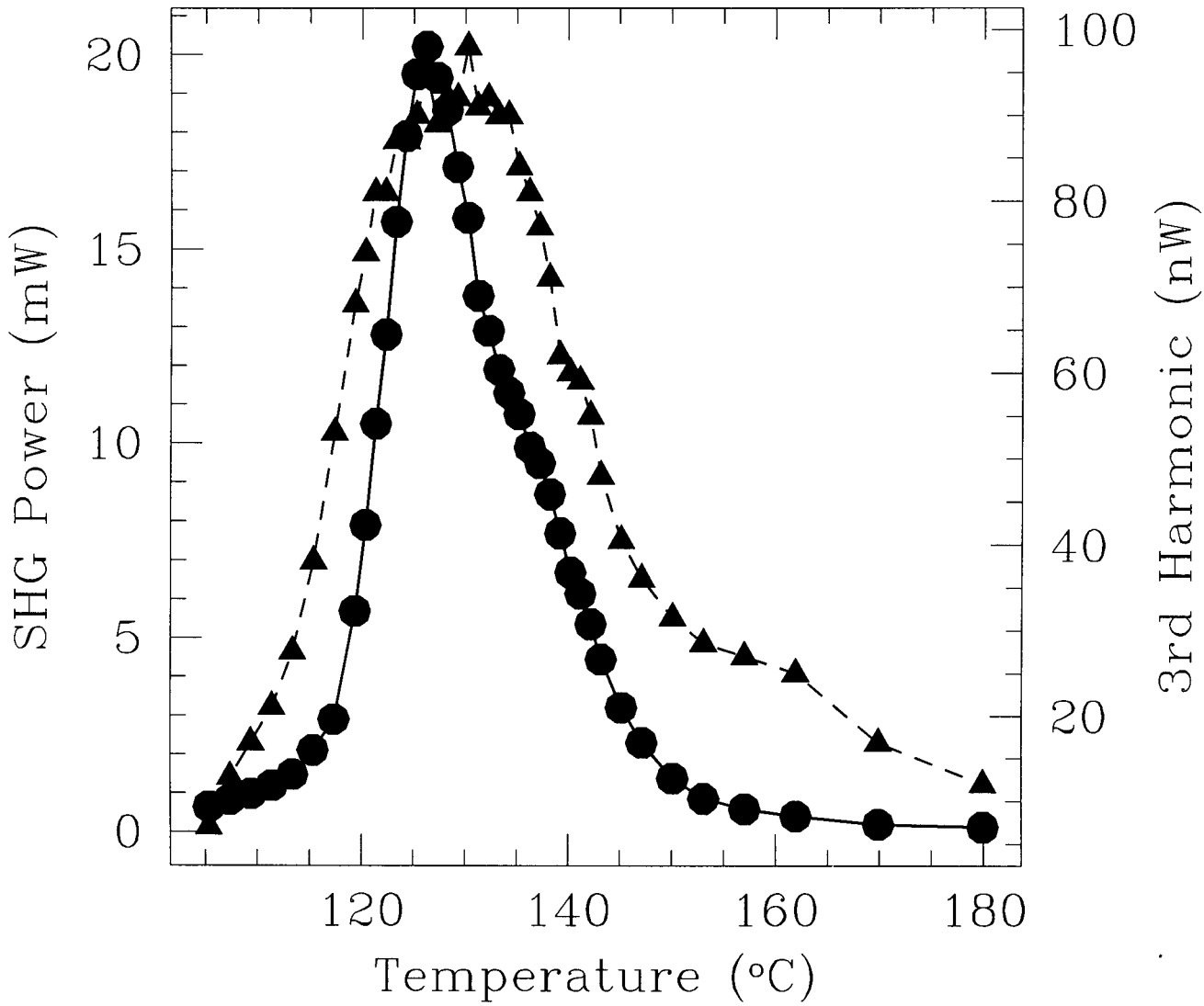

FIG. 5: Temperature tuning curves for the second and third harmonics. The circles represents the 2nd harmonic while the triangles represent the 3rd harmonic.

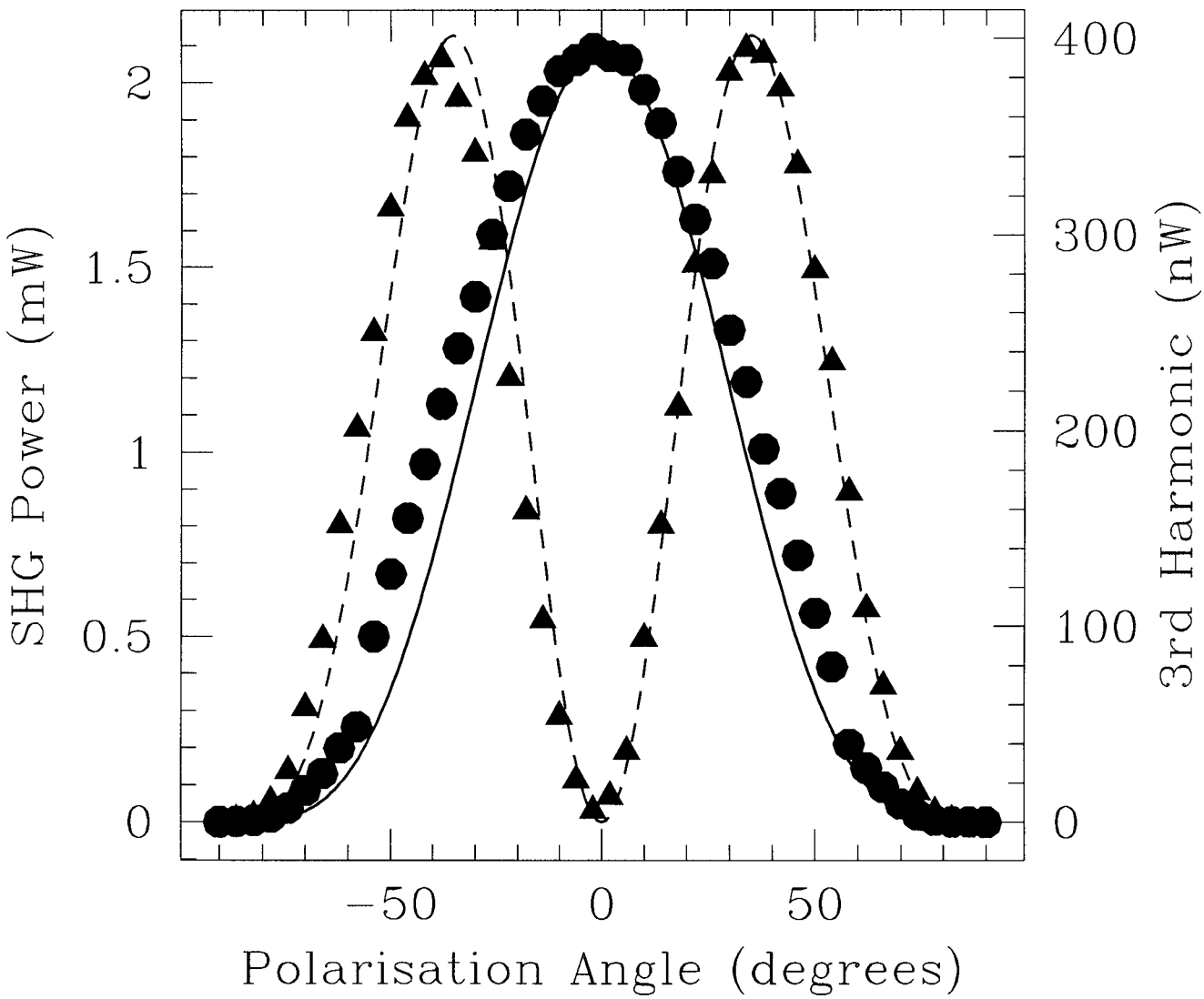

FIG. 6: Angle tuning of the type II third harmonic generation process. The points represent the experimental measurements while the lines represent the theoretical model. Here it can be clearly seen that when the fundamental and 2nd harmonic are vertically polarised no third harmonic light can be seen.

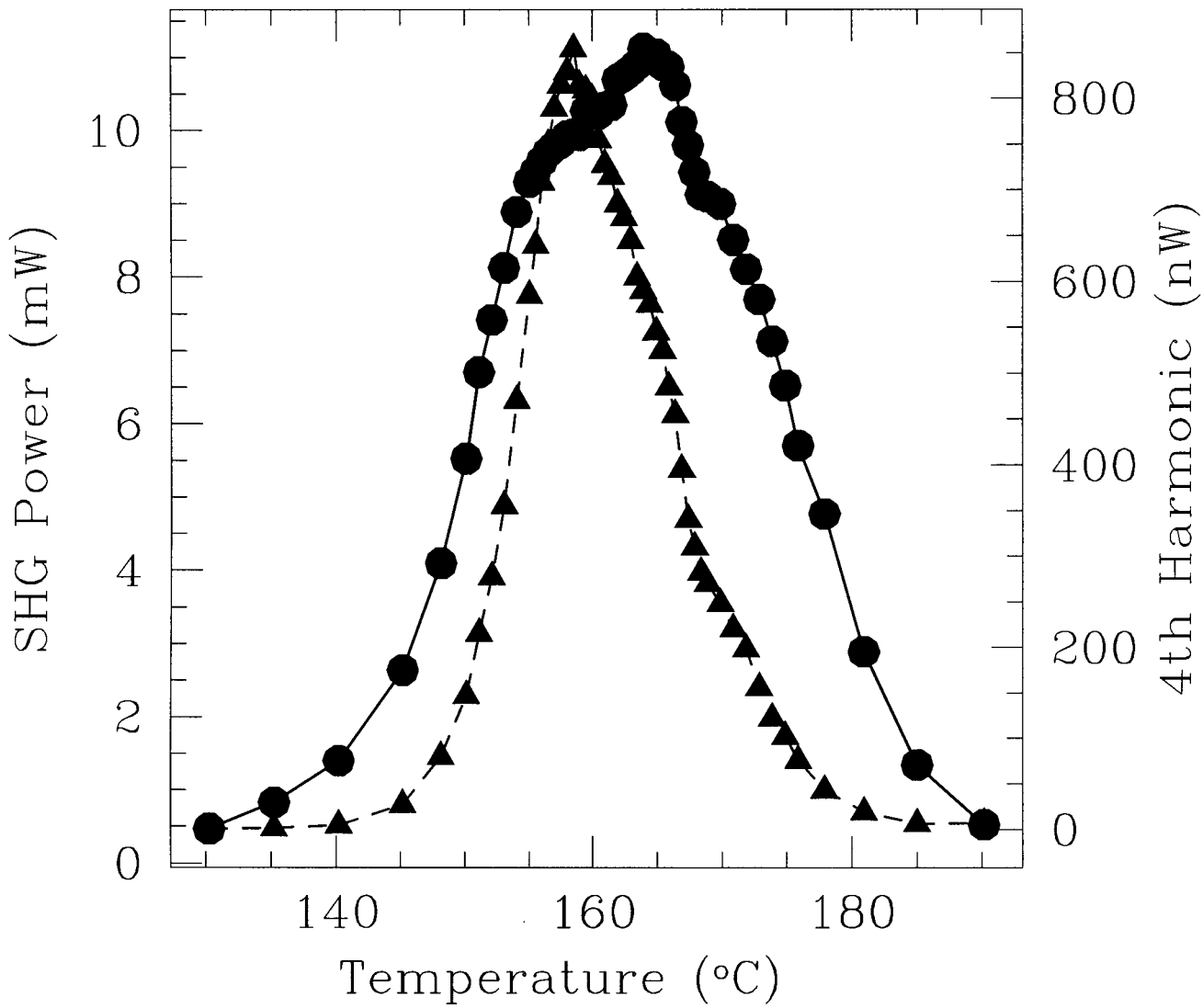

FIG. 7: Temperature tuning curves for the second and fourth harmonics. The circles represents the 2nd harmonic while the triangles represent the 4th harmonic.